

# Isolated lepton events at HERA: SUSY $R$ -parity violation?

S.Y. Choi<sup>1,2,a</sup>, J. Kalinowski<sup>3</sup>, H.-U. Martyn<sup>1,4</sup>, R. Rückl<sup>5</sup>, H. Spiesberger<sup>6</sup>, P.M. Zerwas<sup>1</sup>

<sup>1</sup> Deutsches Elektronen-Synchrotron DESY, 22603 Hamburg, Germany

<sup>2</sup> Physics Department and RIPC, Chonbuk National University, Jeonju 561-756, Korea

<sup>3</sup> Institute of Theoretical Physics, Warsaw University, 00681 Warsaw, Poland

<sup>4</sup> I. Physikalisches Institut, RWTH Aachen, Aachen, Germany

<sup>5</sup> Institut für Theoretische Physik, Universität Würzburg, 97074 Würzburg, Germany

<sup>6</sup> Institut für Physik, Johannes-Gutenberg-Universität Mainz, 55099 Mainz, Germany

Received: 9 January 2007 / Revised version: 27 February 2007 /

Published online: 22 June 2007 – © Springer-Verlag / Società Italiana di Fisica 2007

**Abstract.** Events with an isolated high  $p_T$  lepton, a hadron jet and missing energy as observed in the H1 experiment at HERA, are potentially associated with  $R$ -parity violation in supersymmetric theories. However, stringent kinematic constraints must be fulfilled if the production of supersymmetric particles in  $R$ -parity violating scenarios were the correct path for explaining these puzzling events. A reference point  $\mathbb{R}$  is specified for which these constraints are illustrated and implications of the supersymmetric interpretation for new classes of multi-lepton events are indicated.

## 1 Introduction

Several events with an isolated lepton in association with a hadron jet and missing transverse momentum,

$$e^+p \rightarrow e^+/\mu^+ + \text{jet} + p_T^{\text{miss}} \quad (1)$$

have been observed in the H1 experiment at HERA. For events with the jet transverse momentum larger than 25 GeV, the yield is larger, at a level of  $3.4\sigma$ , than the number expected in the Standard Model [1–3], in which  $W$  production [4, 5], with subsequent leptonic decays, gives rise to these final states. This type of events has been observed in running HERA with positrons but not with electrons. ZEUS, on the other hand, has not reported the observation of excess of such events [6, 7]. A comparison of the H1 and ZEUS data can be found in [8].

A potential interpretation of the events (1) is based on supersymmetric theories incorporating  $R$ -parity violating interactions (for a recent review of  $R$ -parity violating supersymmetry see [9]). Most of the models assume the formation of fairly light stop particles in  $e^+d$  fusion, via the  $R$ -parity violating interaction  $\lambda'_{131}L_1Q_3D_1^c$  in the superpotential, with stops decaying to a  $b$ -jet and a chargino.<sup>1</sup>

<sup>a</sup> e-mail: sychoi@chonbuk.ac.kr

<sup>1</sup> Our discussion applies equally well to scenarios in which a charm squark is produced in  $e^+d$  fusion via the  $\lambda'_{121}$  coupling and decays to a  $s$ -jet and a chargino. However, due to possible strong mixing in the stop sector, the lightest stop can be expected considerably lighter than the charm squark. The models differ in the structure of the subsequent decay chains of the chargino.

(i) Chargino decays to a  $W$ -boson and a neutralino  $\tilde{\chi}_1^0$  have been analyzed in [10, 11], and chargino decays to a lepton and a sneutrino in [11]. However, subsequent neutralino/sneutrino decays generate final states more complex than in (1), unless the neutralino [12] or the sneutrino is assumed to be metastable, decaying outside the detector. Such an interpretation is very unlikely however since the neutralino lifetime for  $\tilde{\chi}_1^0$  decays is bounded from above by the  $\tilde{\chi}_1^0 \rightarrow b\tilde{b} \rightarrow b\nu$  channel mediated by a virtual  $\tilde{b}$ . The size of the partial width, estimated as  $\Gamma(\tilde{\chi}_1^0) \sim 3\alpha_W(\lambda'_{131}/4\pi)m_{\tilde{\chi}_1^0}^5/32\pi m_{\tilde{b}}^4$ , is set by the size of the  $e^+d\tilde{t}$  coupling responsible for the production process, see (3), and the  $\tilde{b}$  mass ( $\alpha_W$  denotes the electroweak  $SU(2)_L$  fine structure constant  $g_2^2/4\pi$ ). Similar consequences can be drawn when a metastable sneutrino  $\tilde{\nu}_\tau$  is the lightest SUSY particle, even if direct  $R$ -parity violating  $\tilde{\nu}_\tau$  couplings are absent, cf. [13, 14]. The sneutrino may decay “back” through the channel  $\tilde{\nu}_\tau \rightarrow \tau\tilde{\chi}_1^+ \rightarrow \tau b\tilde{t} \rightarrow \tau be^+d$  involving virtual intermediate  $\tilde{\chi}_1^+$  and  $\tilde{t}$  states, with  $\Gamma(\tilde{\nu}_\tau) \sim \alpha_W^2(\lambda'_{131}/4\pi)m_{\tilde{\nu}_\tau}^7/256\pi^2m_{\tilde{\chi}_1^+}^2m_{\tilde{t}}^4$ . The estimated decay widths of the two modes,  $\Gamma(\tilde{\chi}_1^0) \sim 1$  eV and  $\Gamma(\tilde{\nu}_\tau) \sim 10^{-3}$  eV, for  $\lambda'_{131} \sim 5 \times 10^{-2}$  and SUSY masses  $\mathcal{O}(100)$  GeV, suggest lifetimes of order  $\sim 10^{-15}$  s and  $\sim 10^{-12}$  s, respectively, much too short for the particles to escape the detector before decay. Alternatively, the experimental analysis of [15] is based on stop decays to on-shell bottom squarks  $\tilde{b}_1$  and  $W$ -bosons, with  $\tilde{b}_1$  decaying through  $R$ -parity

violating coupling to  $d$ -quark and neutrino. Such an explanation of the signature (1) assumes a mechanism for generating a  $\tilde{b}_1$  squark in the mass range of 100 to 200 GeV much lighter than all other squark masses, decaying into the standard experimental channel jet plus missing energy.

- (ii) A different class of models is based on  $\mathbb{R}_p$  violation in both lepton–quark and lepton–lepton interactions. The chargino, generated in the stop decay, decays to a charged slepton and a neutrino, followed by the subsequent slepton  $\mathbb{R}_p$  decay to a lepton + neutrino pair, cf. [16, 17]. This mechanism generates the characteristic final state of (1) as shown in Fig. 1a. The production of the intermediate stop particle is governed by the  $\mathbb{R}_p$  term  $\lambda' L Q D^c$  in the superpotential, and the slepton decay to a lepton + neutrino pair by  $\lambda L L E^c$ . (The slepton may also decay back, with strength  $\lambda'$ , to a top + jet pair.) Moreover, if the chargino decays alternatively to a sneutrino and a charged lepton, the final state, three charged leptons and no missing transverse energy as predicted by the same  $\mathbb{R}_p$  coupling, can be reconstructed *in toto*, Fig. 1b. (Also in this case the lepton pair may be replaced by a jet pair.)

Besides the prediction of additional lepton and jet final states in the second scenario, the clustering of partons and leptons at invariant masses corresponding to the chargino mass in all events, and in addition the sneutrino mass in multi-lepton events, provides powerful internal cross-checks of the SUSY  $\mathbb{R}_p$  interpretation of any events with signature (1). (If the on-shell constraints fail, the escape to virtual intermediate states is hardly a way out as rates fall dramatically in this case.)

The coupling  $\lambda'$  must be sufficiently large, a few  $10^{-2}$  for  $\lambda'_{131}$ , to guarantee the necessary stop production rate. This size can only be maintained if the suppression of rare lepton final states in meson decays is reached either by selection of non-vanishing  $\lambda', \lambda$  couplings or by fine-tuned destructive interference between several  $\lambda', \lambda$  couplings. Though the fine-tuning of order  $10^{-1}$  to  $10^{-2}$  remains moderate, both solutions are based on *ad-hoc* assumptions which superficially lack naturalness.

These general remarks will be illustrated in the analysis of a specific reference point  $\mathbb{R}$  in the next section. Many of the discussions will be generic and the emphasis will not be on the detailed properties of the model but on the general characteristics that can easily be transferred to a wider scenario and to other scenarios. In particular

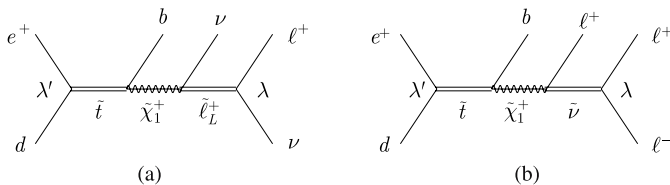


**Fig. 1.** Supersymmetric  $R$ -parity violating interactions generating isolated lepton events

the crucial clustering conditions will apply to any scenario based on stop production in the  $s$ -channel and they are characteristic for a whole class of  $\mathbb{R}_p$  models for the supersymmetric interpretation of the HERA events. The reference point  $\mathbb{R}$  is chosen to develop constraints on the SUSY  $\mathbb{R}_p$  interpretation of experimental data but it should not be mis-interpreted as an outstanding candidate for explaining existing data.

## 2 An $R$ -parity violating stop scenario

The reference point  $\mathbb{R}$  is defined such that stop states are mixed strongly and a rather light  $\tilde{t}_1$  emerges while all the other squark states are heavy. The light chargino and the lightest neutralino are assumed higgsino-like so as to suppress  $\tilde{\chi}_1^+ \rightarrow W^+ \tilde{\chi}_1^0$  decays in the  $\tilde{t}_1$  cascade which, with subsequent  $\mathbb{R}_p$  violating  $\tilde{\chi}_1^0$  decays, would not generate the desired final states. The Higgs mixing parameter  $\tan\beta$  is chosen moderate to allow comparable charged slepton and sneutrino decays of the chargino. ( $R$ -type sneutrinos are assumed to be very heavy and inaccessible.)

Constraints on the  $\lambda'$  and  $\lambda$  couplings in  $\mathbb{R}$  from rare mesonic decays may be illustrated by three important examples [18–20]:

$$\begin{aligned} B_d^0 \rightarrow \mu\mu &: |\lambda'_{131}\lambda_{122}^* + \lambda'_{331}\lambda_{322}^*| \lesssim 3.4 \times 10^{-6} [\tilde{m}/100 \text{ GeV}]^2 \\ B_d^0 \rightarrow \mu e &: |\lambda'_{131}\lambda_{121}^* + \lambda'_{331}\lambda_{321}^*| \lesssim 8.0 \times 10^{-6} [\tilde{m}/100 \text{ GeV}]^2 \\ K_L^0 \rightarrow \mu e &: |\lambda'_{1k1}\lambda_{2k2}^*| \lesssim 3 \times 10^{-7} [\tilde{m}/100 \text{ GeV}]^2, \end{aligned} \quad (2)$$

where  $\tilde{m}$  is the mass of the sparticle involved in the decay. Vastly different  $\lambda'$  and  $\lambda$  values in any product of the couplings or fine-tuning in destructive interferences can suppress all these amplitudes. To illustrate the first point, we may assume  $\lambda'_{131}$  sufficiently large for generating the necessary  $\tilde{t}_1$  rate, and  $\lambda_{322}$  or/and  $\lambda_{321}$  sufficiently large for generating isolated  $\mu$  and  $e$  events (for the sake of simplicity assumed to be equal). The constraints from rare  $B$ -decays can be complied with in this configuration if  $\lambda'_{331}$  and  $\lambda_{122,121}$  are very small. The third condition can be solved in a similar way or by destructive interferences in the amplitudes. Even though such a specific choice may look unnatural, it cannot be refuted by experimental results on the other hand.

Summarizing, the reference point  $\mathbb{R}$  defined in Table 1 does not appear in conflict with experimental data. The  $\mathbb{R}_p$  couplings of the superfields generate interactions in the (s)quark and (s)lepton sectors of the type:

$$\begin{aligned} \lambda'_{131} L_1 Q_3 D_1^c &\Rightarrow \lambda'_{131} (e\tilde{t}d - \nu_e\tilde{b}d + \text{cycled}) \\ \lambda_{322} L_3 L_2 E_2^c &\Rightarrow \lambda_{322} (\tau\tilde{\nu}_\mu\mu - \nu_\tau\tilde{\mu}\mu + \text{cycled}) \\ \lambda_{321} L_3 L_2 E_1^c &\Rightarrow \lambda_{321} (\tau\tilde{\nu}_\mu e - \nu_\tau\tilde{\mu}e + \text{cycled}). \end{aligned} \quad (3)$$

For brevity we use a simplified notation in which fields are supposed to be cycled, with the tilde characterizing the fermion field kept in the middle position.

Masses and mixings generated by this reference point, and relevant for the subsequent discussion, are listed in

**Table 1.** Definition of the reference point  $\mathbb{R}$ . For simplicity, lepton and quark universality is assumed for the SUSY parameters and the mixing of squarks and sleptons, except for stop, is ignored

$\mathbb{R}$ : Parameters	Values
elw gaugino masses	$M_2 = 2M_1 = 1.5$ TeV
higgsino mass	$\mu = 160$ GeV
Higgs mixing	$\tan\beta = 1.5$
scalar lepton masses	$M_L = M_E = 130$ GeV
scalar quark masses	$M_Q = M_U = M_D = 420$ GeV
trilinear $A$ coupling	$A_t = 840$ GeV
$\lambda', \lambda$ couplings	$\lambda'_{131} = 5 \times 10^{-2}$ $\lambda_{322} = \lambda_{321} = \lambda'_{131}$ other $\lambda', \lambda$ very small

**Table 2.** Masses and mixings at the reference point  $\mathbb{R}$ . The stop mixing matrix  $U_{\tilde{t}}$  relates the stop mass and current states,  $(\tilde{t}_1, \tilde{t}_2)_i = [U_{\tilde{t}}]_{i\alpha}(\tilde{t}_L, \tilde{t}_R)_\alpha$ , and the chargino/neutralino mixing matrices relate their mass and current states correspondingly

$\mathbb{R}$ : Observables	Masses and mixing elements
stop masses	$m[\tilde{t}_{1/2}] = 203/609$ GeV
stop mixing	$[U_{\tilde{t}}]_{11} = -0.71$
slepton/ sneutrino masses	$m[\tilde{\ell}_L/\tilde{\nu}] = 133/123$ GeV
chargino masses	$m[\tilde{\chi}_{1/2}^\pm] = 156/1505$ GeV
chargino mixings	$[U_{L/R}]_{11} = -0.049/-0.068$
neutralino masses	$m[\tilde{\chi}_{1/2/3/4}^0] = 152/160/753/1505$ GeV
neutralino mixings	$[N]_{11/2/3/4} = -0.070/0.058/-0.71/0.70$

Table 2. These values are compatible with the bounds on masses and mixings from LEP, Tevatron and HERA [21]. If interpreted strictly within the MSSM, the parameters would lead to too low a mass of the lightest Higgs boson; however, this mass can be raised beyond the LEP limit in extended theories [22] without affecting the mass and mixing parameters of Table 2 significantly, cf. [23].

### 3 Stop phenomenology at HERA

The production cross section of stop particles at HERA, cf. Fig. 1, is given in the narrow-width approximation by

$$\begin{aligned} \sigma(e^+p \rightarrow \tilde{t}_1) &= \hat{\sigma}_0(e^+d \rightarrow \tilde{t}_1) f_d \left( \frac{m_{\tilde{t}_1}^2}{s} \right) \\ \hat{\sigma}_0(e^+d \rightarrow \tilde{t}_1) &= \frac{\pi}{4m_{\tilde{t}_1}^2} |\lambda'_{131}|^2 |[U_{\tilde{t}}]_{11}|^2 \end{aligned} \quad (4)$$

with the  $d$ -parton density  $f_d$  in the proton evaluated at  $x = m_{\tilde{t}_1}^2/s$ . For the  $\mathbb{R}$  parameter set introduced above and the MRST2004 parametrization of the parton densities [24], the numerical value of  $\sigma(e^+p \rightarrow \tilde{t}_1) = 0.54$  pb leads to a sample of about ninety  $\tilde{t}_1$  events for an integrated luminosity of  $\int \mathcal{L} = 160$  pb $^{-1}$ . The luminosity

roughly corresponds to the  $e^+p$  data presented by the HERA experiments [1–3, 6, 7].

Since the  $t\tilde{\chi}_1^0$  decay channel is kinematically inaccessible,  $\tilde{t}_1$  particles decay to nearly 100% into  $b\tilde{\chi}_1^+$  final states, as indicated in Fig. 1; remnant  $\tilde{R}_p$  decays to  $e^+/\tau^+d$  are reduced to a level of 3% as a result of the small  $\lambda'_{131/331}$  couplings compared with the gauge coupling.

Also the subsequent chargino  $\tilde{\chi}_1^+$  decays follow the standard path to  $\tilde{\ell}_L^+\nu_\ell$  and  $\tilde{\nu}\ell^+$  final states since the chargino decay to  $W^+\tilde{\chi}_1^0$  is strongly suppressed  $\sim (m_{\tilde{\chi}_1^+} - m_{\tilde{\chi}_1^0})^5$  in the higgsino region with nearly degenerate  $\tilde{\chi}_1^+/\tilde{\chi}_1^0$  states, i.e.  $\Delta m_{\tilde{\chi}} \simeq 4$  GeV in  $\mathbb{R}$ . The partial widths are given by

$$\begin{aligned} \Gamma(\tilde{\chi}_1^+ \rightarrow \tilde{\ell}_L^+\nu_\ell/\tilde{\nu}\ell^+) &= \frac{\alpha}{16\sin^2\theta_W} m_{\tilde{\chi}_1^\pm} \\ &\times \left[ 1 - m_{\tilde{\ell}_L/\tilde{\nu}}^2/m_{\tilde{\chi}_1^\pm}^2 \right]^2 |[U_{L/R}]_{11}|^2. \end{aligned} \quad (5)$$

To generate a sufficiently large number of isolated lepton plus missing  $p_T$  events, the Higgs mixing parameter  $\tan\beta$  cannot be much larger than unity; this is required by the electroweak  $D$  term  $m_{\tilde{\nu}}^2 - m_{\tilde{\ell}_L}^2 = m_W^2 \cos 2\beta$  as well as the ratio of mixing elements  $[U_L]_{11}/[U_R]_{11} \sim 1/\tan\beta$ . The branching ratio for charged slepton final states amounts to 21% so that a significant number of sneutrino final states is predicted in the  $\mathbb{R}$  environment. Reducing  $\tan\beta$  further leads to near balance between charged and neutral sleptons.

For the decays of the charged sleptons and sneutrinos a variety of channels may be open. In addition to the leptonic  $\tilde{R}_p$  decays, hadronic  $\tilde{R}_p$  decays and standard gaugino decays to  $\tilde{\chi}_1^0$  may be observed, with  $\tilde{\chi}_1^0$  finally decaying to leptons and hadrons through  $\tilde{R}_p$  interactions mediated by a virtual  $\tilde{b}$  state:

$$\begin{aligned} \tilde{\ell}_L^+ &\rightarrow e^+\nu_\mu, e^+\nu_\tau, \mu^+\nu_\mu, \mu^+\nu_\tau; t\bar{b}; \ell^+\tilde{\chi}_1^0 \\ \tilde{\nu}_\ell &\rightarrow e^-\mu^+, e^-\tau^+, \mu^-\mu^+, \mu^-\tau^+; d\bar{b}; \nu_\ell\tilde{\chi}_1^0. \end{aligned} \quad (6)$$

The branching ratios depend strongly on the details of the parameter choice, apparent from the partial widths:

$$\Gamma(\tilde{\ell}_L \rightarrow \ell\nu/\tilde{\nu} \rightarrow \ell\ell') = \frac{|\lambda|^2}{16\pi} m_{\tilde{\ell}_L/\tilde{\nu}} \quad (7)$$

$$\Gamma(\tilde{\ell}_L \rightarrow t d/\tilde{\nu} \rightarrow b d) = \frac{3|\lambda'|^2}{16\pi} m_{\tilde{\ell}_L/\tilde{\nu}} \left[ 1 - m_{t/b}^2/m_{\tilde{\ell}_L/\tilde{\nu}}^2 \right]^2 \quad (8)$$

$$\begin{aligned} \Gamma(\tilde{\ell}_L \rightarrow \ell\tilde{\chi}_1^0/\tilde{\nu} \rightarrow \nu\tilde{\chi}_1^0) &= \frac{\alpha}{4\sin^2 2\theta_W} |N_{12}c_W + N_{11}s_W|^2 \\ &\times m_{\tilde{\ell}_L/\tilde{\nu}} \left[ 1 - m_{\tilde{\chi}_1^0}^2/m_{\tilde{\ell}_L/\tilde{\nu}}^2 \right]^2. \end{aligned} \quad (9)$$

In the reference scenario selectrons and  $e$ -sneutrinos decay into hadrons, but the other  $\mu, \tau$  type sleptons decay to leptons. Standard neutralino decays are also suppressed due to the reduced phase-space if the neutralino mass is close

**Table 3.** The slepton/sneutrino decay modes of the chargino and the experimentally observable final states in the  $\mathbb{R}$  scenario. Estimates of the combined branching ratios for the  $\tilde{t}_1$  decays to the observable final states are listed in the last column. (The top quark in  $\tilde{e}_L^+ \rightarrow t\bar{d}$  is virtual as  $m_{\tilde{e}_L} < m_t$ .)

$\tilde{\chi}_1^+$ decay	$\tilde{t}_1 \rightarrow b\tilde{\chi}_1^+ \rightarrow b\tilde{\ell}_L^+\nu$ and $b\tilde{\nu}\ell^+$		$e^+p \rightarrow \tilde{t}_1$ final state	Estimated fractions (%)	
	$\lambda_{322}$	$\lambda_{321}$			
$\tilde{e}_L^+\nu_e$	—	—	$t^*\bar{d}$	$jjW^+b\cancel{E}_T$	7.0
$\tilde{\mu}_L^+\nu_\mu$	$\mu^+\nu_\tau$	$e^+\nu_\tau$	—	$\mu^+j\cancel{E}_T$ and $e^+j\cancel{E}_T$	3.5 and 3.5
$\tilde{\tau}_L^+\nu_\tau$	$\mu^+\nu_\mu$	$e^+\nu_\mu$	—	$\mu^+j\cancel{E}_T$ and $e^+j\cancel{E}_T$	3.5 and 3.5
$\tilde{\nu}_e e^+$	—	—	$d\bar{b}$	$e^+jjj$	23.0
$\tilde{\nu}_\mu \mu^+$	$\mu^-\tau^+$	$e^-\tau^+$	—	$\mu^-\mu^+\tau^+j$ and $e^-\mu^+\tau^+j$	11.5 and 11.5
$\tilde{\nu}_\tau \tau^+$	$\mu^-\mu^+$	$e^-\mu^+$	—	$\mu^-\mu^+\tau^+j$ and $e^-\mu^+\tau^+j$	11.5 and 11.5

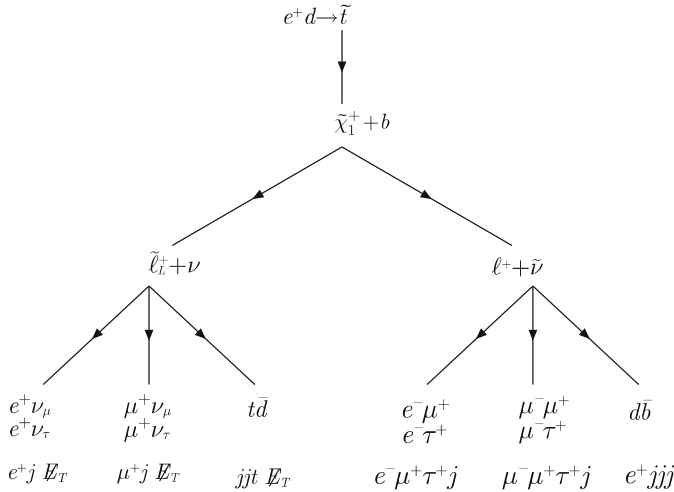


**Fig. 2.** Mixed  $R$ -parity conserving and  $R$ -parity violating decays of the lighter top squark  $\tilde{t}_1$  which give rise to multi-lepton and jet final states with missing transverse momentum (*left cascade*) due to escaping neutrinos

to the slepton/sneutrino masses and if the neutralino is higgsino-like.

The chargino decay modes in the  $\mathbb{R}$  scenario are summarized in Table 3, leading to the experimentally observable final states indicated in the two branches of Fig. 2 for charged leptons and sneutrinos. All multi-lepton events in  $\mathbb{R}$  contain  $\tau^+$ 's in the final state.

A large variety of experimental signatures emerges from the model, with no overwhelming preference for a particular channel, but large uncertainties due to the choice of mass, mixing and  $\lambda'$ ,  $\lambda$  parameters. The table should therefore not be interpreted as a quantitative prediction but rather as a listing of interesting signatures to be searched for experimentally.

## 4 Kinematical constraints

In on-shell  $\tilde{t}_1$  production in  $e^+d$  collisions, the  $\tilde{t}_1$  mass determines the value  $x$  of the target  $d$  parton,

$$x = m_{\tilde{t}_1}^2 / s. \quad (10)$$

The 4-momentum of the stop quark, traveling along the proton direction, is predicted to be

$$p_{\tilde{t}_1} = p_e + \left( m_{\tilde{t}_1}^2 / s \right) p_p \quad (11)$$

in obvious notation for the momenta of  $\tilde{t}_1$ , positron and proton. Energy and 3-momentum of  $\tilde{t}_1$  along the proton axis are fixed in the laboratory frame by

$$\begin{aligned} E_{\tilde{t}_1} &= E_e + \left( m_{\tilde{t}_1}^2 / s \right) E_p \\ p_{\tilde{t}_1}^z &= -E_e + \left( m_{\tilde{t}_1}^2 / s \right) E_p, \end{aligned} \quad (12)$$

where  $E_e$  and  $E_p$  are the HERA energies for the positron and proton beams, respectively. These relations for the stop energy and momentum serve as basis for evaluating the kinematical constraint equations which follow from the on-shell condition for  $\tilde{\chi}_1^+$ .

The technique of constraint equations applies to all scenarios discussed above (and universally, *mutatis mutandis*, to all SUSY  $\mathbb{R}_p$  scenarios in which  $\tilde{t}_1$  decays proceed to the final state (1) through cascades involving intermediate supersymmetric particles like  $\tilde{\chi}_1^+$ ). Using the  $\tilde{t}_1$  4-momentum from (12) and the measured  $b$ -jet energy  $E_b$  and longitudinal  $z$ -momentum  $p_b^z$  along the proton direction, the  $\tilde{\chi}_1^+$  mass condition  $m_{\tilde{\chi}_1^+}^2 = (p_{\tilde{t}_1} - p_b)^2$  can be cast in the form

$$m_{\tilde{\chi}_1^\pm}^2 = m_{\tilde{t}_1}^2 [1 - (E_b - p_b^z) / 2E_e] - 2E_e (E_b + p_b^z). \quad (13)$$

With the *a priori* unknown stop and chargino masses, each event with measured values of  $b$ -jet energy and longitudinal momentum defines, according to (13), a line in the  $(m_x^2, m_y^2)$  plane, the coordinates labeled by  $(m_x^2, m_y^2)$ .

Lines corresponding to the signal events must cross at the single point corresponding to the true values of stop and chargino masses  $(m_x^2, m_y^2) = (m_{\tilde{t}_1}^2, m_{\tilde{\chi}_1^\pm}^2)$ , if the considered  $\mathbb{R}_p$  scenario is the correct interpretation of the data. This is demonstrated in Fig. 3a for the reference point  $\mathbb{R}$ .

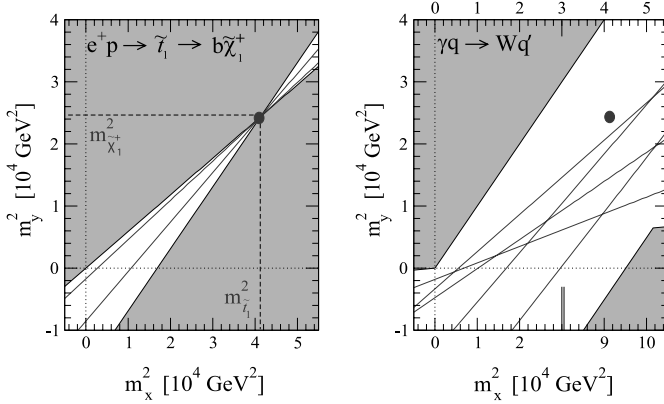


**Fig. 3.** *Left:* Lines corresponding to  $\tilde{R}_p$  signal events. All signal lines must lie within the double cone. The *dot* corresponds to the signal point for the true mass values,  $m_x^2 \rightarrow m_{\tilde{t}_1}^2$  and  $m_y^2 \rightarrow m_{\tilde{\chi}_1^\pm}^2$ . *Right:* Lines corresponding to background events from  $W$ -photoproduction  $\gamma q \rightarrow Wq'$ . The kinematically excluded regions bounded by *black solid lines* are shaded. (Note that the lower  $x$ -axis is cut to accommodate the forbidden wedge on the right.)

All allowed signal lines in the mass plane are located within the double cone formed by the line with slope = 1 and cutting the  $m_y^2$ -axis at the minimum value  $-(m_{\tilde{t}_1}^2 - m_{\tilde{\chi}_1^\pm}^2)$ , and the line crossing the origin with slope  $m_{\tilde{\chi}_1^\pm}^2/m_{\tilde{t}_1}^2$ , both intercept and slope given by the true mass values. The opening angle of the cone increases apparently with the  $\tilde{t}_1 - \tilde{\chi}_1^\pm$  mass gap.

On the other hand, lines corresponding to background events do not cross at a single point but rather form an irregular mesh over the  $(m_x^2, m_y^2)$  plane. This is shown in Fig. 3b for a few examples for which the jet parameters are identified with values derived from  $W$ -photoproduction  $\gamma q \rightarrow Wq'$ . Inserting jet energy and momentum for a sample of events apparently does not lead to any clustering of the solutions (in contrast to the signal lines), reflecting that the process does not proceed through resonance formation. For  $W$ -photoproduction the lines fill the area between (and including) the double-cone of maximum  $\gamma q$  invariant mass,  $M_{\gamma q}^2 = s$ , and the line corresponding to the degenerate double-cone for minimum  $\gamma q$  invariant mass,  $M_{\gamma q}^2 = M_W^2$ .

Apparent from Figs. 1a and b and Table 3, many more consistency conditions can be derived from the leptons and jets in the final state.

Two examples are provided by the first and fourth row in Table 3. The  $\tilde{e}_L^+$  events in the first row must cluster at the invariant mass

$$M[jt] = m_{\tilde{e}_L} \quad (14)$$

while the  $\tilde{\nu}_e$  events in the fourth row must cluster at the triple point

$$M[jj] = m_{\tilde{\nu}_e}$$

$$\begin{aligned} M[e^+ jj] &= m_{\tilde{\chi}_1^+} \\ M[e^+ jjj] &= m_{\tilde{t}_1}. \end{aligned} \quad (15)$$

Moreover, since the  $\nu_\tau$  3-momentum can be reconstructed fully in single  $\tau$  events, the last two rows of Table 3 accounting for all sneutrino decays, must fulfill a large set of constraint equations. This may be illustrated by analyzing the  $\mu\mu$  chain of the last row in Table 3:

$$\begin{aligned} M[\mu\mu] &= m_{\tilde{\nu}_\tau} \\ M[\tau^+ \mu\mu] &= m_{\tilde{\chi}_1^+} \\ M[j\tau^+ \mu\mu] &= m_{\tilde{t}_1} \end{aligned} \quad (16)$$

and analogously for the other chains. Particularly appealing is the requirement of clustering for the 2-lepton and 3-lepton invariant masses at the  $\tilde{\nu}$  and  $\tilde{\chi}_1^+$  masses.

It should also be noted that the transverse energies of the  $b$ -jets in the laboratory cluster for  $\tilde{t}_1 \rightarrow b\tilde{\chi}_1^+$  decays at the maximum possible value

$$\max[E_T^b] = (m_{\tilde{t}_1}^2 - m_{\tilde{\chi}_1^+}^2)/2m_{\tilde{t}_1} \quad (17)$$

as a result of the well-known transverse Jacobian peak.

## 5 Conclusions

In this brief note we have examined necessary requirements which the interpretation of isolated lepton events with large missing transverse momentum and a hadron jet at HERA must comply with in the context of  $R$ -parity violating supersymmetric interactions. Independent of the specific reference point used in this note merely to illustrate the analysis in detail, two generic implications have emerged from the study:

- Kinematical constraint equations relate the observed jet and lepton energies and momenta with masses of stop, chargino and sneutrino, and clusters of invariant masses must be observed experimentally.
- $R$ -parity violating couplings connect leptons and sleptons of different charges and species. This implies that also events including multi-lepton final states and  $\tau^+$  leptons should be observed.

The lifetime of meta-stable neutralinos and sneutrinos is estimated to be very likely too short to provide a possible alternative to the generic type of scenarios analyzed above.

*Acknowledgements.* We should like to thank G. Brandt for providing us with the  $W$ -photoproduction events. A communication on the Higgs sector by F. Richard is gratefully acknowledged. The work was supported in part by the Korea Research Foundation Grant (KRF-2006-013-C00097), by KOSEF through CHEP at Kyungpook National University, by the Polish Ministry of Science and Higher Education Grant No 1 P03B 108 30, by the German Ministry of Education and Research (BMBF) under contract number 05HT6WWA, and

by the EC contract MTKD-CT-2005-029466. S.Y.C. is grateful for support during his visit to DESY.

## References

1. H1 Collaboration, V. Andreev et al., Phys. Lett. B **561**, 241 (2003) [arXiv:hep-ex/0301030]
2. D. South, Proceedings, DIS2006, Tsukuba, 2006, <http://www-conf.kek.jp/dis06/doc/WG3/ew06-south.pdf>
3. H1 Collaboration, Contributed paper to ICHEP, Moscow, 2006, <http://www-h1.desy.de/psfiles/confpap/ICHEP2006/H1prelim-06-162.ps>
4. K.P. Diener, C. Schwanenberger, M. Spira, Eur. Phys. J. C **25**, 405 (2002) [arXiv:hep-ph/0203269]
5. P. Nason, R. Rückl, M. Spira, J. Phys. G **25**, 1434 (1999) [arXiv:hep-ph/9902296]
6. ZEUS Collaboration, S. Chekanov et al., Phys. Lett. B **559**, 153 (2003) [arXiv:hep-ex/0302010]
7. ZEUS Collaboration, Contributed paper to ICHEP, Moscow, 2006, <http://www-zeus.desy.de/physics/phch/conf/ichep06/hq2/1/ZEUS-prel-06-012.pdf>
8. C. Diaconu, arXiv:hep-ex/0610041, to be published in Proc. the XXXIII International Conference On High Energy Physics, Moscow, 2006
9. R. Barbier et al., Phys. Rep. **420**, 1 (2005) [arXiv:hep-ph/0406039]
10. H1 Collaboration, A. Aktas et al., Eur. Phys. J. C **36**, 425 (2004) [arXiv:hep-ex/0403027]
11. ZEUS Collaboration, S. Chekanov et al., arXiv:hep-ex/0611018
12. T. Kon, T. Kobayashi, S. Kitamura, Phys. Lett. B **376**, 227 (1996) [arXiv:hep-ph/9601338]
13. D. South, <http://www-conf.kek.jp/dis06/transparencies/WG3/ew-south.pdf> and arXiv:hep-ex/0607020, in: Proc. the XIV International Workshop on Deep Inelastic Scattering, Tsukuba, 2006, p. 325
14. E. Sauvan, <http://www-conf.kek.jp/dis06/transparencies/summary/ew/pl-sauvan.pdf> and arXiv:hep-ph/0607273, in: L. Bellagamba, E. Sauvan, H. Spiesberger, Proc. the XIV International Workshop on Deep Inelastic Scattering, Tsukuba, 2006, p. 867
15. H1 Collaboration, A. Aktas et al., Phys. Lett. B **599**, 159 (2004) [arXiv:hep-ex/0405070]
16. J. Kalinowski, R. Rückl, H. Spiesberger, P.M. Zerwas, DESY Internal Note, 1997, available on [http://wwwthep.physik.uni-mainz.de/~hspiesb/publications\\_pre97/rpv\\_hera\\_97.pdf](http://wwwthep.physik.uni-mainz.de/~hspiesb/publications_pre97/rpv_hera_97.pdf)
17. C. Diaconu, J. Kalinowski, T. Matsushita, H. Spiesberger, D.S. Waters, Proceedings, 3rd UK Workshop on HERA Physics, Durham, J. Phys. G **25**, 1412 (1999) [arXiv:hep-ph/9901335]
18. J.H. Jang, J.K. Kim, J.S. Lee, Phys. Rev. D **55**, 7296 (1997) [arXiv:hep-ph/9701283]
19. H.K. Dreiner, G. Polesello, M. Thormeier, Phys. Rev. D **65**, 115006 (2002) [arXiv:hep-ph/0112228]
20. R. Van Kooten, Proc. 4th Flavor Physics and CP Violation Conference (FPCP 2006), Vancouver BC, arXiv:hep-ex/0606005
21. L. Bellagamba, arXiv:hep-ex/0611012
22. S.F. King, S. Moretti, R. Nevzorov, Phys. Lett. B **634**, 278 (2006) [arXiv:hep-ph/0511256]
23. S.Y. Choi, H.E. Haber, J. Kalinowski, P.M. Zerwas, arXiv:hep-ph/0612218
24. A.D. Martin, W.J. Stirling, R.S. Thorne, Phys. Lett. B **636**, 259 (2006) [arXiv:hep-ph/0603143]